Optimal electrode selection for multichannel EEG based detection of auditory cortex and brainstem auditory steady–state responses

Bram Van Dun[a)] and Jan Wouters

ExpORL,

Katholieke Universiteit Leuven,

Herestraat 49/721,

B-3000 Leuven,

Belgium

Marc Moonen

ESAT–SCD/SISTA,

Katholieke Universiteit Leuven,

Kasteelpark Arenberg 10,

B-3001 Leuven,

Belgium

(Dated: October 13, 2008)

Abstract

Auditory steady–state responses (ASSRs) in EEG measurements are currently used for reliable hearing threshold estimation at audiometric frequencies. Especially hearing impaired newborns benefit from this technique, as it allows for a better diagnosis and hence a hearing aid can be better fitted at an early age. Unfortunately measurement duration is still long for clinical widespread use. This paper evaluates the practical performance of a multichannel EEG processing strategy based on a detection theory approach. This multichannel strategy significantly reduces measurement time. Based on eight–channel EEG measurements of ten normal–hearing adults, an optimal electrode selection is determined for ASSRs with frequencies between 80 and 110 Hz originating mainly from the brainstem. In combination with the multichannel processing scheme, a minimum set of electrodes is obtained that provides a close–to–optimal hearing threshold estimate of all subjects. This minimum electrode setup, together with the multichannel signal processing, is significantly more robust against artifacts, effectively doubling the number of significant ASSR detections when compared with a single channel measurement. Similarly, an optimal electrode set is determined for 10 Hz ASSRs mainly originating beyond the brainstem. This minimum set allows to record close–to–optimal signal–to–noise ratios within 80% of the subjects.

PACS numbers: 43.64.Ri, 43.66.Yw, 43.66.Sr

I. INTRODUCTION

In 1994 the Joint Committee on Infant Hearing (JCIH) stated that universal detection of infants with a hearing loss is recommended before the age of three months (Joint Committee on Infant Hearing, 1995). Therefore, the need for objective audiometric techniques has greatly increased over the last decade. As the number of early hearing screened newborns grows worldwide, an appropriate clinical response to the need for rehabilitation of hearing problems is necessary. An effective treatment may consist in the use of a hearing aid. However, the fitting of this device requires a frequency specific estimation of the newborn's hearing thresholds. These estimates can be provided using auditory steady–state response (ASSR) detection long before first behavioral thresholds can be obtained. Unfortunately, a reliable ASSR–based hearing threshold estimation procedure with adults already takes 45 minutes, and can last several hours with newborns (Luts *et al.*, 2006). The measured signals are often corrupted by artifacts due to the newborn's uncontrolled activity. The general aim is thus to increase robustness against artifacts and to reduce the measurement time. Before actual studies can be carried out on infants, the proposed techniques are evaluated on adults because behavioral hearing thresholds can easily be determined with adults and hence a reference is obtained for the application in the infant population.

The ASSR is an electrophysiological response of the brain evoked by acoustic stimuli. These stimuli are generally based on amplitude and/or frequency modulated sinusoidal carriers. The carriers stimulate specific parts of the cochlea, while the modulations activate certain parts of the auditory system. The appearance of the modulator in the EEG can be used as a label for the carrier. The first significant ASSR study was conducted by Galambos *et al.* (1981) with modulation frequencies of 40 Hz. Subsequently, extensive research showed that the ASSR can indeed provide an objective and frequency specific way to determine

[a)] Also at ESAT–SCD/SISTA, Katholieke Universiteit Leuven, Kasteelpark Arenberg 10, B-3001 Leuven, Belgium; Electronic address: `bram.vandun@med.kuleuven.be`; URL: `http://www.kuleuven.be/exporl`

reliable hearing thresholds, both applicable to adults and infants (we refer to Picton *et al.* (2003) for an extensive overview).

Many research studies have focused on optimizing detection of ASSRs. First, different stimulus types have been investigated. Amplitude and/or frequency modulated stimuli are most widely accepted (John *et al.*, 2001b). In addition, the application of other stimuli has been studied, such as stimuli with exponential modulation envelopes (John *et al.*, 2002), broadband and band–limited noise (John *et al.*, 2003), stimuli composed of several carriers modulated with the same modulation frequency (Stürzebecher *et al.*, 2001), and complex stimuli with broader frequency spectra (Riquelme *et al.*, 2006; Stürzebecher *et al.*, 2006). In general, responses are more difficult to detect as the stimuli become more frequency specific. Second, normal averaging has been compared with weighted averaging and artifact rejection (John *et al.*, 2001a). Third, the possibility to increase the efficiency of ASSR detection by means of multichannel EEG recordings has been evaluated (van der Reijden *et al.*, 2004; Van Dun *et al.*, 2007a,b). Finally, several statistical decision criteria have been studied: tests that use spectral phase information, spectral amplitude information, or both; tests that evaluate only the first harmonic of the response (Cebulla *et al.*, 2001; Dobie and Wilson, 1996) and recently, tests that include higher harmonics for response detection (Cebulla *et al.*, 2006).

Most of these studies however are based on EEG obtained from subjects who were instructed to relax or sleep. These experiment conditions can be considered as almost ideal. In practice, however, and especially when e.g. newborns are tested, numerous artifacts prevent a successful measurement unless one takes appropriate measures against these artifacts. This can be achieved by using artifact rejection or weighted averaging (John *et al.*, 2001a). The downside of these techniques is the unacceptably long measurement time in the case only one EEG channel is used for EEG signal recording, as data blocks severely corrupted with artifacts are entirely discarded or are not allowed to contribute much to the final result. Therefore, other techniques have been researched that are more robust against artifacts. These techniques should allow to detect significantly more responses in artifactual EEG without extending measurement time.

The Cz–Oz or Cz–neck derivations are the most commonly used derivations for adults (John *et al.*, 2001a; Lins and Picton, 1995; Luts and Wouters, 2005). The choice for these derivations lies in the general experience that the mean ASSR thresholds are smaller for these EEG derivations. This experience is confirmed for the Cz–Oz derivation by van der Reijden *et al.* (2004), who use a multichannel setup to search for the EEG derivations offering the largest signal–to–noise (SNR) values and thus the smallest ASSR thresholds for adults. van der Reijden *et al.* (2004) also indicate that this Cz–Oz derivation does not always guarantee the largest SNR and that sometimes other derivations (like e.g. Cz–mastoid, Cz–Pz, and Cz–neck) could offer larger SNRs. This is backed by the observation that ASSR thresholds (and their SNRs) show large variations across subjects (John *et al.*, 2001a; Lins and Picton, 1995; Luts and Wouters, 2005). The problem is that the derivation with the largest SNR is subject dependent and cannot be predicted beforehand. Recording EEG using multiple derivations simultaneously, combined with appropriate multichannel processing, is required to select the 'best' channel (or combination of channels) for as many subjects as possible.

This paper evaluates the practical performance of a multichannel processing strategy based on a detection theory approach, when applied to adults. It is based on eight–channel EEG measurements of ten normal–hearing adults. The results serve as an intermediate step for application of the multichannel processing to infants. First, the EEG derivation with the best estimation of the behavioral hearing threshold for ASSRs originating mainly from the brainstem is determined (modulation frequencies between 80 and 110 Hz in this paper). For ASSRs originating mainly from the auditory cortex (modulation frequency of 10 Hz in this paper), the EEG derivation with the largest SNR is determined similarly. Then, the minimum EEG channel combination is determined for brainstem ASSRs with a close–to–optimal estimation of the behavioral hearing threshold for as many subjects as possible. As a practical application of this result, the robustness of this minimum set to artifacts is investigated. Similarly, for auditory cortex ASSRs, the minimum EEG channel combination is determined that provides a close–to–largest SNR for a maximum number of subjects.

II. THEORETICAL BACKGROUND

ASSRs are difficult to detect due to noise originating from sources both inside and outside the skull. As a result, clinical measurements can last unacceptably long. Specifically designed signal processing techniques may reduce this measurement time and may increase the robustness against suddenly emerging short–termed energetic artifacts that appear frequently in ASSR measurements.

This section gives a summary of a multichannel signal processing technique described in detail in Van Dun *et al.* (2008a). Its rationale is based on a concept from detection theory, namely the *sufficient statistic*. This sufficient statistic can exploit spatio-temporal information present in the EEG measurements. The resulting approach can be linked with the multichannel Wiener filter (MWF) (Simmer *et al.*, 2001; Van Dun *et al.*, 2007b) and with independent component analysis (ICA) (Hyvärinen *et al.*, 2001; Van Dun *et al.*, 2007a). This detection theory based technique offers an improved detection of ASSRs in artifact–rich EEG compared to techniques that process single channel EEG.

A. ASSR data model

A general ASSR data model can be given as

$$\boldsymbol{Z} = \alpha \boldsymbol{S} \boldsymbol{D}^T + \boldsymbol{N} \tag{1}$$

with $\boldsymbol{Z}^{n\times m}$ an observation matrix, α a scalar representing the ASSR source amplitude proportional to the applied stimulus intensity, $\boldsymbol{S}^{n\times 2}$ a desired signal matrix with columns representing the ASSR (sinusoid & cosinusoid, oscillating at the known modulation frequency), $\boldsymbol{D}^{m\times 2}$ a steering matrix, $\boldsymbol{N}^{n\times m}$ an additive noise matrix, n the number of data points, and m the number of measured EEG channels.

In (1), given only $\boldsymbol{Z}$ and $\boldsymbol{S}$, $\alpha\boldsymbol{D}$ and $\boldsymbol{N}$ can be estimated using a QR–factorisation:

$$\overbrace{\left[\, \boldsymbol{s}_1^{n\times 1} \;\; \boldsymbol{s}_2^{n\times 1} \;\; \boldsymbol{Z}^{n\times m} \,\right]}^{\boldsymbol{S}} = \boldsymbol{Q}^{n\times(m+2)} \boldsymbol{R}^{(m+2)\times(m+2)} \tag{2}$$

with

$$\boldsymbol{Q} = \begin{bmatrix} \boldsymbol{s}_1 & \boldsymbol{s}_2 & \boldsymbol{Q}_*^{n\times m} \end{bmatrix}, \qquad \boldsymbol{R} = \begin{bmatrix} 1 & 0 & \hat{\boldsymbol{d}}_1^T \\ 0 & 1 & \hat{\boldsymbol{d}}_2^T \\ \boldsymbol{0} & \boldsymbol{0} & \boldsymbol{R}_*^{m\times m} \end{bmatrix} \tag{3}$$

$\boldsymbol{Z}$ can then be written as

$$\boldsymbol{Z} = \overbrace{\begin{bmatrix} \boldsymbol{s}_1 & \boldsymbol{s}_2 \end{bmatrix}}^{\boldsymbol{S}} \overbrace{\begin{bmatrix} \hat{\boldsymbol{d}}_1^T \\ \hat{\boldsymbol{d}}_2^T \end{bmatrix}}^{\hat{\boldsymbol{D}}^T} + \overbrace{\boldsymbol{Q}_*\boldsymbol{R}_*}^{\hat{\boldsymbol{N}}} \tag{4}$$

where $\hat{\boldsymbol{D}}$ and $\hat{\boldsymbol{N}}$ are the estimates provided for $\alpha\boldsymbol{D}$ and $\boldsymbol{N}$.

A physical interpretation is provided as follows. The ASSR generator has an unknown source amplitude α which depends on the stimulus level. After propagation through the skull, the distribution of the recorded ASSR on the electrodes, present in the observation matrix $\boldsymbol{Z}$, can be described by the steering matrix $\boldsymbol{D}$. The steering matrix $\boldsymbol{D}$, in contrast with the additive EEG noise, is usually assumed to be stationary as it is merely a representation of the source position, its directivity pattern, the electrode positions, and the propagation attenuation from source to electrode. Physically no measurable delay occurs between the ASSR source and the electrodes (order of nanoseconds). Therefore the ASSR delay difference and hence the ASSR phase difference between electrodes is assumed to be zero. On the other hand, the delay between ASSR stimulus and response is measurable (order of milliseconds) but unknown to the observer as it depends on several physical parameters of the subject. The ASSR phase φ at the electrodes is thus unknown but equal in all channels.

Formula (1) can then be rewritten as

$$\boldsymbol{Z} = \alpha\boldsymbol{S} \overbrace{\begin{bmatrix} \cos\varphi \\ \sin\varphi \end{bmatrix}}^{\boldsymbol{D}^T} \boldsymbol{d}^T + \boldsymbol{N} \tag{5}$$

$$= \alpha\boldsymbol{s}\boldsymbol{d}^T + \boldsymbol{N} \tag{6}$$

where now $\boldsymbol{s}$ and $\boldsymbol{d}$ are vectors, and φ corresponds to the ASSR phase.

The phase φ can be estimated based on (4),

$$\hat{\varphi} = \arg\left\{ \max_{\varphi} \begin{bmatrix} \cos\varphi & \sin\varphi \end{bmatrix} \hat{\boldsymbol{D}}^T (\hat{\boldsymbol{N}}^T \hat{\boldsymbol{N}})^{-1} \hat{\boldsymbol{D}} \begin{bmatrix} \cos\varphi \\ \sin\varphi \end{bmatrix} \right\} \tag{7}$$

The estimated phase $\hat{\varphi}$ expresses the direction that maximizes the projection of the observation matrix $\boldsymbol{Z}$ onto the desired signal $\boldsymbol{S}[\cos\varphi \;\; sin\varphi]^T$ as $\hat{\boldsymbol{D}} = \boldsymbol{Z}^T \boldsymbol{S}$. Based on $\hat{\varphi}$, a rotation transformation is applied to $\hat{\boldsymbol{D}}$,

$$\hat{\boldsymbol{d}} = \hat{\boldsymbol{D}} \begin{bmatrix} \cos\hat{\varphi} \\ \sin\hat{\varphi} \end{bmatrix} \tag{8}$$

such that the estimated steering matrix $\hat{\boldsymbol{D}}$ is transformed into an estimated steering vector $\hat{\boldsymbol{d}}$.

A spatio–temporal noise covariance matrix $\boldsymbol{K}^{mn \times mn}$ can be defined as

$$\boldsymbol{K} = \mathcal{E}\{\boldsymbol{n}\boldsymbol{n}^T\} \tag{9}$$

with $\boldsymbol{n} = \mathrm{vec}(\boldsymbol{N})$. Here $\mathcal{E}\{\cdot\}$ is the expected value operator and the $\mathrm{vec}(\cdot)$ operator stacks the columns of a matrix $\boldsymbol{X}$ into one column vector $\boldsymbol{x} = \mathrm{vec}(\boldsymbol{X})$.

If the spatial and temporal correlations are separable, as will be observed here, the spatio–temporal noise covariance matrix $\boldsymbol{K}$ can be written as (Johnson and Dudgeon, 1993)

$$\boldsymbol{K} = \boldsymbol{K}_{\mathrm{spat}} \otimes \boldsymbol{K}_{\mathrm{temp}} \tag{10}$$

where $\otimes$ represents the Kronecker product, with a spatial noise covariance matrix $\boldsymbol{K}_{\mathrm{spat}}^{m \times m}$, representing the noise correlation across the different channels,

$$\boldsymbol{K}_{\mathrm{spat}} = \mathcal{E}\{\boldsymbol{N}^T \boldsymbol{N}\} \tag{11}$$

and a temporal noise covariance matrix $\boldsymbol{K}_{\mathrm{temp}}^{n \times n}$, representing the correlation of noise samples within the same channel,

$$\boldsymbol{K}_{\mathrm{temp}} = \mathcal{E}\{\boldsymbol{N}\boldsymbol{N}^T\} \tag{12}$$

Based on (4) the noise covariance matrices can be estimated as

$$\hat{\boldsymbol{K}}_{\mathrm{spat}} = \hat{\boldsymbol{N}}^T \hat{\boldsymbol{N}} \qquad \hat{\boldsymbol{K}}_{\mathrm{temp}} = \hat{\boldsymbol{N}} \hat{\boldsymbol{N}}^T \tag{13}$$

B. Detection theory: detecting signals with unknown amplitude in noise

Detection theory is a means to quantify the ability to discern between signal and noise (Green and Swets, 1966). Here, a *sufficient statistic* $\Upsilon(\boldsymbol{z})$ is defined,

$$\Upsilon(\boldsymbol{z}) = \boldsymbol{z}^T \boldsymbol{K}^{-1} \tilde{\boldsymbol{s}} \tag{14}$$

with a target signal $\tilde{\boldsymbol{s}}$ having an unknown amplitude α, and $\boldsymbol{K}$ the covariance matrix of the noise $\boldsymbol{n}$ that corrupts the observation vector $\boldsymbol{z}$,

$$\boldsymbol{z} = \alpha \tilde{\boldsymbol{s}} + \boldsymbol{n} \tag{15}$$

A sufficient statistic theoretically captures best the amount of useful target signal $\tilde{\boldsymbol{s}}$ in the vector $\boldsymbol{z}$ containing the observations. A decision threshold η for $\Upsilon(\boldsymbol{z})$ can be determined by specifying a false–alarm probability. This threshold η decides whether the observation vector $\boldsymbol{z}$ contains the target signal $\tilde{\boldsymbol{s}}$ or not.

C. A detection theory framework for ASSR processing

The ASSR signal model of (6), can be rewritten as

$$\boldsymbol{z} = \alpha \overbrace{\boldsymbol{d} \otimes \boldsymbol{s}}^{\tilde{\boldsymbol{s}}} + \boldsymbol{n} \tag{16}$$

with $\boldsymbol{z} = \mathrm{vec}(\boldsymbol{Z})$ and $\boldsymbol{n} = \mathrm{vec}(\boldsymbol{N})$ respectively.
The sufficient statistic formula (14) can be applied here (by identifying (15) with (16)),

$$\Upsilon_A(\boldsymbol{z}) = \boldsymbol{z}^T \boldsymbol{K}^{-1} \tilde{\boldsymbol{s}} \tag{17}$$

Replacing $\boldsymbol{K}$, by using (10), and $\tilde{\boldsymbol{s}}$ by using (16), one can write

$$\Upsilon_A(\boldsymbol{z}) = \boldsymbol{z}^T (\boldsymbol{K}_{\mathrm{spat}} \otimes \boldsymbol{K}_{\mathrm{temp}})^{-1} (\boldsymbol{d} \otimes \boldsymbol{s}) \tag{18}$$

$$= \boldsymbol{s}^T \boldsymbol{K}_{\mathrm{temp}}^{-T} \boldsymbol{Z} \boldsymbol{K}_{\mathrm{spat}}^{-1} \boldsymbol{d} \tag{19}$$

Substituting the estimates based on (2), (3), (4), (7), (8), and (13) then leads to a sufficient statistic $\hat{\Upsilon}_A(\boldsymbol{z})$ suitable for ASSR detection,

$$\hat{\Upsilon}_A(\boldsymbol{z}) = \begin{bmatrix} \cos\hat{\varphi} & \sin\hat{\varphi} \end{bmatrix} \boldsymbol{S}^T \hat{\boldsymbol{K}}_{\text{temp}}^{-T} \boldsymbol{Z} \hat{\boldsymbol{K}}_{\text{spat}}^{-1} \hat{\boldsymbol{D}} \begin{bmatrix} \cos\hat{\varphi} \\ \sin\hat{\varphi} \end{bmatrix} \tag{20}$$

When the EEG (noise) is stationary over all channels throughout the measurement, the covariance matrix $\boldsymbol{K}$ is constant too. When it is assumed that the noise characteristics change over time, $\boldsymbol{K}$ cannot be considered constant anymore and so (20) needs to be modified. If the noise in $\boldsymbol{Z}$ is stationary only in blocks of T samples (rows) and if the noise is assumed uncorrelated between such blocks, then $\Upsilon_A(\boldsymbol{z})$ can be calculated as the sum of the sufficient statistics $\Upsilon_{A,i}(\boldsymbol{z}_i)$, for the individual blocks $\boldsymbol{Z}_i$, i.e.

$$\Upsilon_A(\boldsymbol{z}) = \sum_{i=1}^{\frac{n}{T}} \boldsymbol{s}_i^T \boldsymbol{K}_{\text{temp},i}^{-T} \boldsymbol{Z}_i \boldsymbol{K}_{\text{spat},i}^{-1} \boldsymbol{d} \tag{21}$$

$$= \sum_{i=1}^{\frac{n}{T}} \Upsilon_{A,i}(\boldsymbol{z}_i) \tag{22}$$

For each $\Upsilon_{A,i}(\boldsymbol{z}_i)$ an approximation as in (20) can then be substituted.

D. Detection using the Fast Fourier Transformation (FFT)

In many ASSR studies an objective procedure is adapted, where an FFT analysis is carried out prior to response detection (John and Picton, 2000; Lins and Picton, 1995; Luts *et al.*, 2006; Valdes *et al.*, 1997). The detection is then based on the ratio between the response power P_r at the modulation frequency and the mean noise power σ^2 in M neighboring frequency bins at each side,

$$\frac{P_r}{\sigma^2} = \frac{a_{\text{response}}^2}{\frac{1}{M}\sum_{p=1}^{M} a_{\text{noise},p}^2} \tag{23}$$

with a_{response} the amplitude at the modulation frequency and $a_{\text{noise},p}$ the noise amplitude in the p–th adjacent frequency bin (John and Picton, 2000).

For brainstem responses (with modulation frequencies between 80 and 110 Hz), M is taken equal to 120 (approximately 3.7 Hz on each side). For auditory cortex responses (10 Hz), M is taken equal to 60 (approximately 1.85 Hz on each side).

III. METHODS

Two types of studies will be described here: one based on ASSRs mainly evoked in the brainstem (modulation frequencies between 80 and 110 Hz) and one based on ASSRs mainly evoked in the auditory cortex (10 Hz).

The 80–110 Hz range is the frequency region of interest for hearing threshold determination (Picton *et al.*, 2003). Several studies focus on the sources of these ASSRs. Herdman *et al.* (2002) suggest that 88 Hz ASSRs are mainly generated in the brainstem. Kuwada *et al.* (2002) indicate that ASSRs with modulation frequencies below 80 Hz mainly originate in the auditory cortex. Above 80 Hz, there appears to be at least two generators that are likely subcortical. This is confirmed by Purcell *et al.* (2004) who use response latencies to derive the source locations. They conclude that for modulation frequencies above about 75 Hz, most of the ASSR is generated in the brainstem. Above 95 Hz, the source lies entirely in the brainstem. As a result, responses to stimuli modulated with frequencies between 80 and 110 Hz are referred to as 'responses mainly evoked in the brainstem'.

The modulation frequency of 10 Hz is chosen because its relevance for speech envelope modulations and speech perception (Shannon *et al.*, 1995). When lowering the modulation frequency of the stimulus, the main source of the ASSR shifts more to the auditory cortex. According to Herdman *et al.* (2002), the main source can be found in the auditory cortex, but a source originating from the brainstem may still be present. This is supported by Purcell *et al.* (2004), showing that the brainstem still contributes at lower modulation frequencies, but with the main source of the low–frequency ASSR placed in the auditory cortex. Responses to 10 Hz–modulated stimuli are therefore referred to as 'responses mainly evoked in the auditory cortex'.

For both studies, 10 normal hearing subjects (8 male, 2 female) with mean age 28.2 years (range 22–32 years) were selected. Their hearing thresholds did not exceed 20 dBHL on the octave audiometric frequencies. All experiments were carried out in a double–walled soundproof room with Faraday–cage. Subjects were instructed to lie down on a bed and relax or sleep for the brainstem study in Section III.A, and to stay awake by watching a movie for the auditory cortex study in Section III.B. Lights were switched off. This procedure was repeated a number of weeks later to collect both test and retest data.

Kendall jelly snap electrodes were placed on the positions described in Table I according to the international 10–20 system (Malmivuo and Plonsey, 1995). This configuration was chosen similar to van der Reijden *et al.* (2004) with some extra channels added to ensure a symmetrical configuration of all electrodes. They were placed on the subject's scalp after the skin was abraded with Nuprep abrasive skin prepping gel. A conductive paste was used to keep the electrodes in place and to avoid that inter–electrode impedances exceeded 5 kΩ at 30 Hz. The electrodes were connected to a low–noise eight–channel Jaeger–Toennies amplifier. Each EEG channel was amplified (× 50,000) and bandpass filtered between 70 and 170 Hz (6 dB/octave) for the brainstem study in Section III.A, and between 1 and 30 Hz (6 dB/octave) for the auditory cortex study in Section III.B. The sampling rate was set equal to 1000 Hz, and downsampled afterwards to 250 Hz. No artifact rejection was applied initially, but a threshold was determined offline that rejected around 10 % of the recorded data blocks ('epochs') that exceeded this threshold. All separate acoustic stimuli were calibrated at 70 dBSPL, using a Brüel & Kjær Sound Level Meter 2260 in combination with a 2–cc coupler DB0138 and an artificial ear 4152. All stimuli were presented to the subject and amplified EEG signals were recorded using the SOMA program from Van Dun *et al.* (2008b) and an RME multichannel soundcard.

It is stressed that all possible measures have been taken to avoid false responses not originating from statistical noise effects (the relative number of false responses originating from statistical noise is allowed to be 5 %). Measures to avoid additional false responses include appropriate shielding of stimulus devices and electrodes, filtering prior to downsampling,

and adequate separation of stimulus and electrode cables. The absence of false responses was regularly checked by applying the stimuli to a simulated 'deaf' subject (by blocking the ear canal of the subject using ear plugs).

A. Brainstem stimulation

Two combined stimuli with four 100% amplitude modulated (AM) and 20% frequency modulated (FM) carrier frequencies each, were applied to each ear. The carrier frequencies were the same for both ears, namely 0.5, 1, 2, and 4 kHz. The modulation frequencies were chosen close to respectively 82, 90, 98, and 106 Hz for the left ear, and 86, 94, 102, and 110 Hz for the right ear. These modulation frequencies were adjusted to ensure that a non–fractional number of modulation cycles fitted into one data block ('epoch') of 1.024 seconds. For example, 82 Hz is converted into $\frac{\text{round}(82*1.024)}{1.024}$ Hz (John and Picton, 2000). Throughout the rest of the manuscript, one will refer to the non–adjusted frequencies for conciseness.

For Sections IV.A.1 and IV.A.2, stimuli were applied at a stepwise decreasing intensity from 60 to 10 dBSPL, and lowered by 10 dB after a trial of approximately 10 minutes per intensity (36 sweeps, each sweep lasting 16.384 seconds). After EEG data collection, each separate channel, or each combination of channels, was reduced to 32 sweeps, using an artifact rejection threshold that removed exactly 4 sweeps per channel (or per combination of channels). Artifact rejection for multichannel data (i.e. a combination of channels) implies the removal of all simultaneous epochs over different channels to preserve correlation over simultaneous channels.

For the analysis of robustness against artifacts in Section IV.A.3, the EEG data from the previous paragraph is used together with extra measurements that emphasized the occurence of artifacts. Subjects were instructed to sit on a chair, and carried out a repeated series of movements in cycles of approximately 6 seconds while the two combined stimuli described above were applied at an intensity of 30 dBSPL. Measurements were 32 sweeps long. No

artifact rejection was applied. The movements were carried out in the following order: look up, down, left, and right. This procedure served as a controlled generator of artifacts on all channels due to muscle activity and electrode cable movement.

B. Auditory cortex stimulation

In contrast with the ASSRs generated mainly in the brainstem (Dimitrijevic *et al.*, 2002; Herdman and Stapells, 2001; Luts and Wouters, 2005), the use (and consequently their mutual interactions) of simultaneous stimuli with different modulation frequencies at 40 Hz and below has not yet been thoroughly documented (Armstrong and Stapells, 2007). Therefore, only one carrier was modulated (instead of eight as in Section III.A), which implies that only one ear was stimulated.

Speech–weighted LIST noise from Van Wieringen and Wouters (2008) was 100 % amplitude modulated with an adjusted modulation frequency close to 10 Hz. The resulting stimulus was applied to the ear with the smallest pure–tone average (PTA), with an intensity of 50 and of 70 dBSPL. Multichannel EEG recordings had a length of 23 sweeps, reduced to 20 sweeps by removing epochs that exceeded the calculated artifact rejection threshold (per channel or per combination of channels), similar to Section III.A.

IV. RESULTS

This section addresses the following questions:

- What is the most appropriate single EEG channel to record brainstem ASSRs and auditory cortex ASSRs respectively?
- What is the most appropriate combination of multiple EEG channels to record brainstem ASSRs and auditory cortex ASSRs respectively?
- Does the side of stimulation influence the conclusions resulting from the questions stated above?

A. Brainstem stimulation

All results in this section are based on the concept of difference scores. A *difference score* is the difference (in dB) between ASSR thresholds (in dBSPL) and behavioral thresholds (in dBSPL). The difference score is used in various ASSR studies (Dimitrijevic *et al.*, 2002; Herdman and Stapells, 2001; Luts and Wouters, 2005). In this study, it allows to combine the available SNR data at six different intensities into one quantitative value. It averages out the variation in behavioral thresholds between subjects and between test sessions within the same subject.

The *ASSR threshold* is defined as the lowest intensity that still produces an ASSR at the corresponding modulation frequency. In the current study this definition is more strict to avoid false detections. A threshold (in dBSPL) is only accepted as threshold if at more than half of the levels (in steps of 10 dBSPL) up to 60 dBSPL a threshold is obtained. For example, one does not define a threshold at 30 dBSPL in the case stimulus levels at 30 and 40 dBSPL show a response, but those at 50 and 60 dBSPL do not. However, if a response is found at 20, 30, and 40 dBSPL, the ASSR threshold is defined at 20 dBSPL. If no threshold is found at 60 dBSPL, the ASSR threshold in this case is defined at 70 dBSPL.

First, parts of the EEG data are presented using SNRs. Then, the conversion to difference scores is justified. The rest of this section will present the results using difference scores.

1. Separate channels

For each EEG channel, Table II displays the mean SNRs (and standard deviations) of the eight modulation frequencies, together with the root–mean–square (RMS) values of the noise between 77 and 115 Hz with the modulation frequencies omitted, when stimulating at 30 dBSPL. It shows the means over 10 subjects, with the test and retest data averaged out for each subject (test–retest not significant over all intensities, $p = 0.404$, no interactions). For conciseness, the values at other intensities (60 to 40, 20, and 10 dBSPL) are not shown.

When the difference scores over all frequencies and all subjects are compared with the SNRs over all frequencies and all subjects, the following Spearman correlations r_s are obtained per stimulus intensity ($p < 0.001$): $r_s = -0.110$ (10 dBSPL), $r_s = -0.378$ (20 dBSPL), $r_s = -0.676$ (30 dBSPL), $r_s = -0.707$ (40 dBSPL), $r_s = -0.678$ (50 dBSPL), and $r_s = -0.573$ (60 dBSPL). The strong correlations just above ASSR hearing threshold seem to justify the use of difference scores instead of SNRs per intensity. The test–retest statistic for difference scores is not significant ($p = 0.439$, no interactions), similar to the test–retest statistic of the SNRs. Difference scores obtained from the same subject can thus be averaged.

Figure 1 shows the mean difference scores (and their standard deviations) per EEG channel for all eight modulated carrier frequencies. Difference scores vary significantly over channels ($p = 0.004$). Comparing pairwise (with Bonferroni correction, $p < 0.05$), channel 1 has significantly better difference scores than channels 3, 6, 7, and 8, channel 3 has significantly better difference scores than channel 6, channel 4 has significantly better difference scores than channels 7 and 8. There is an interaction between subjects and channels ($p = 0.028$). This indicates a significant difference is present between the best channels of one subject compared to the best channels of another subject. Optimal recording results at one particular predefined EEG channel will not be obtained for all subjects.

There is no significant difference ($p \geq 0.05$) between frequencies and between left–right presentation over all channels. Only one other interaction effect is present, namely between channels and left–right application ($p = 0.006$). In Figure 1 it is indicated within which channels a significant difference between application on the left ear and application on the right ear is present. Electrodes placed on the right hemisphere will produce difference thresholds that are significantly smaller for carrier frequencies that are applied to the right ear. A similar, but somewhat smaller effect can be observed for the left hemisphere. The effects described here, significantly present on channels 2, 3, 4, and 6, are confirmed on all these channels by six out of ten subjects. Nine out of ten subjects show these effects on at least three of the four significant channels.

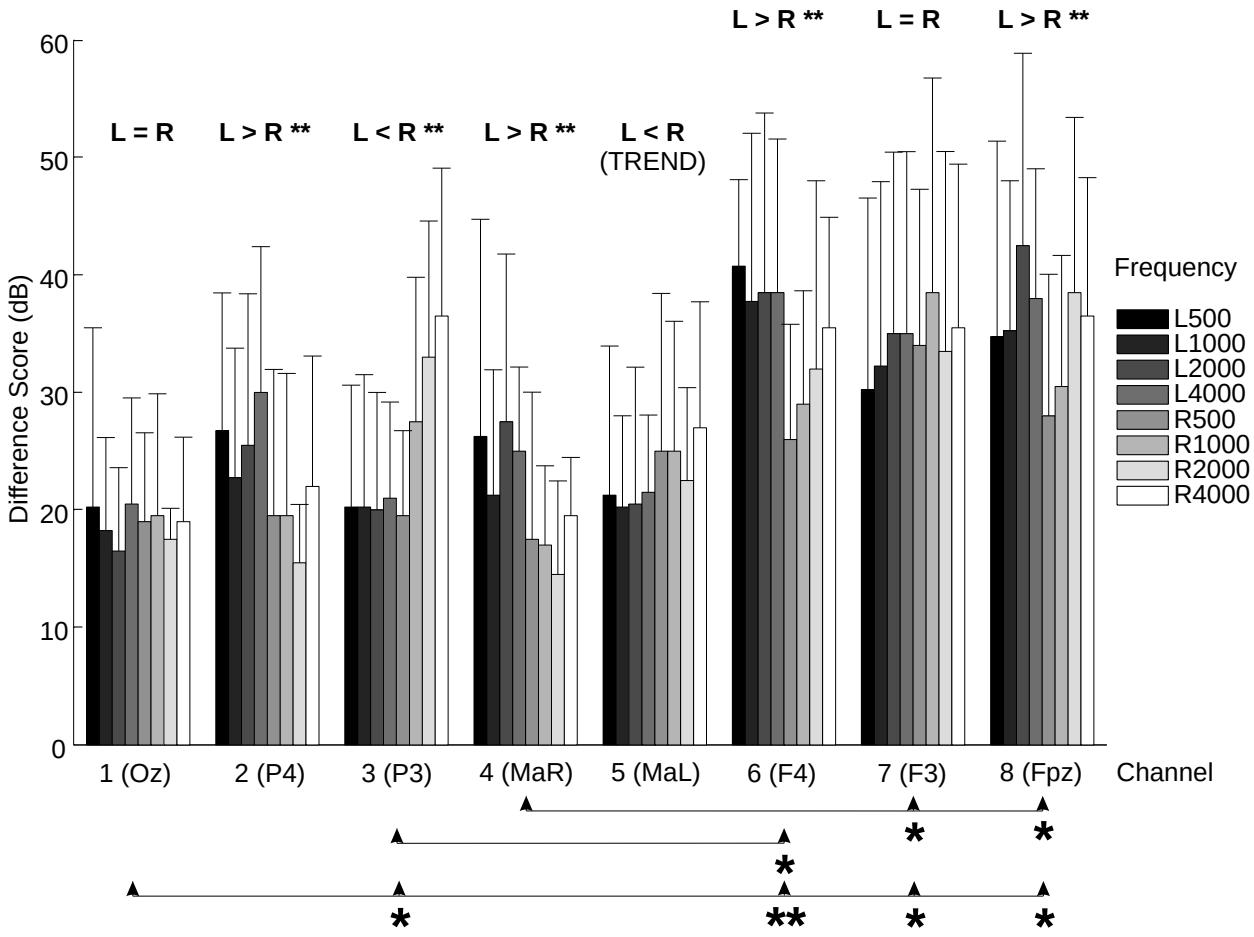

FIG. 1. For each channel from Table I, the mean difference scores (and standard deviations) are displayed for all modulated carriers (500, 1000, 2000, and 4000 Hz, left and right). Above each cluster of bars, the relation between carriers applied to the left ear (L) and the right ear (R) is shown. Under each cluster of bars, a comparison between channels is displayed. If a statistical difference is present, this is indicated with * ($0.05 > p \geq 0.01$) and ** ($0.01 > p \geq 0.001$). A trend is considered present if $0.1 > p \geq 0.05$.

If only three electrodes are available for placement, according to Table I, the best positions for the active and the reference electrodes would be the vertex (Cz) and the inion (Oz), which corresponds to channel 1. This channel returns significantly smaller difference scores than four other channels, including all channels with electrodes on the front side of the head. The side of stimulation is not of significant importance for this channel.

2. Combination of channels

The previous section presented the data of all individual channels from Table I and resulted in an appropriate single channel for smallest difference scores. This section will show the optimal combination of these channels for maximum detection performance (in terms of smallest difference scores), valid for as many subjects as possible and with the restriction that as few electrodes as possible are actually employed. Channels are combined using the detection theory based multichannel processing technique described in Section II. Basically this technique is weighting each channel optimally such that the combined result has the theoretically largest SNR for the ASSR one is looking for (Van Dun *et al.*, 2007b, 2008a).

All 255 ($2^8 - 1$) combinations of the eight EEG channels in Table I are subject to analysis. Channels are combined using (20). Adding extra channels increases the number of detections. The number of extra channels to be added is limited however, as the number of both true and false detections increases. To keep under control the number of false detections, i.e. detections originating from noise only (kept at 5 % in this study), detection decision thresholds have to be tightened accordingly. In theory, a Bonferroni correction should be applied. Practically, this correction is too strict. A detection threshold η is calculated using 'noise' frequencies with no response present. These 'noise' frequencies are selected close to the modulation frequencies that could contain a response (e.g. 1 Hz smaller). For calculation of the noise estimate, frequency bins with a response are removed. By selecting the 95 percentile of this distribution of $\Upsilon_A(\boldsymbol{z})$ values that are calculated on 'noise' frequencies, the practical detection threshold η is found. This is done for each of the 255 combinations.

For each of the 10 subjects (both test and retest), difference scores of eight modulated carrier frequencies are calculated for all 255 combinations. No significant difference between test and retest is found ($p = 0.754$). Therefore, for each subject a difference score average is available per frequency and per combination ($10 \times 255 \times 8$ difference scores in total).

The difference scores of most combinations do not have a normal distribution across subjects. Multivariate analysis requires data with a normal distribution. We follow the nonparametric analysis described in van der Reijden *et al.* (2005), in which outliers are not an issue and equal weights are given to the combinations from each subject regardless of his/her average difference scores.

a. Constructing a top–ten list of combinations

For each of ten subjects, a top–ten list is made of ten combinations with the smallest frequency–averaged difference scores. Five ties are included, limited to the same number of combined channels. This implies that when e.g. channel combination [1,4,8] is ranked 10th, channel combination [3,6,7] with the same difference score is still included, while channel combination [2,3,4,5] (also with the same difference score) is not, as this combination requires one extra electrode which would be less practical. In this particular case, the top–ten list thus contains 105 combinations. Next, the number of times a particular combination appears in the lists is summed over the subjects. The numbers of times the combinations occur are summarized into the histogram in Figure 2. This histogram is then subjected to further analysis to identify any highranking combinations that are dominant in these subjects and that will therefore suffice to record the ASSR efficiently.

The average chance level $\bar{d}$ to appear in the top–ten list is $\bar{d} = \frac{105}{255} = 0.412$. Monte Carlo simulations are used to find the upper limit U of the 95 % confidence interval of the 95 percentile of this distribution d (Press *et al.*, 1992). Therefore, with a reliability of 95 %, a specific combination can only appear more than U times by chance in less than 5 % of the cases. Practically, 1000 distributions d_i are constructed. From each distribution d_i, the 95 percentile P_i^{95} is determined. This returns 1000 values P_i^{95}. A 95 % confidence interval (and its upper limit U) can be calculated of its mean value $\bar{P}^{95}$. Each distribution d_i, containing 5000 instances N_j, is constructed as follows. Out of 255 possible combinations (represented by values between 1 and 255, each corresponding to a particular combination), a selection

S_j of 105 random combinations is made. An arbitrary combination c_j is chosen and the number of appearances N_j of this combination c_j among selection S_j is counted. Instance N_j is one of the 5000 instances that the distribution d_i is built up with. As a validation, the mean values $\bar{d}_i$ are indeed all close to $\frac{105}{255}$. The upper limit U is equal to 2. All values above $U = 2$ in the histogram of Figure 2 (depicted by the dark bars) are thus particular combinations not appearing by chance ($p = 0.05$), with a confidence of 95 %.

The channel combinations in Figure 2 that appear more than $U = 2$ times in the top–ten list with the smallest difference scores over all subjects, are: [1] [1,3] [1,4] [1,5] [1,8] [4,5] [1,3,4] [1,3,8] [1,2,3,4,8]. This series is also displayed in the fourth column of Table III. This result seems promising as these combinations generally appear to contain channels with the smallest difference scores (Figure 1). However, a comparison of the test and retest data shows that the test–retest reproducibility of individual combinations in the top–ten list is low. For the test data the withheld combinations are: [2] [1,2] [1,3] [1,5] [1,6] [1,8] [4,7] [1,2,4] [1,3,7] [1,2,3,4]. For the retest data these are: [1] [1,3] [1,4] [4,5] [1,3,4]. This non–reproducability effect is mainly caused by the fact that a large number (i.e. 255) combinations are candidates for the top–ten list. By focusing on the individual channels appearing in the combinations, this test–retest difference may be reduced.

b. Relative contribution of each channel to a top–ten list

The relative contribution of each individual channel to the top–ten lists described in the previous section is an indicator of the importance of each individual channel. For each subject, the number of appearances of a particular channel in the subject's top–ten list is counted and divided by the number of channels in the top–ten list. In this way, the test and retest are not significantly different ($p = 0.509$, no interactions). The test–retest combined data are displayed per subject in Figure 3, together with the total relative contribution per channel over all subjects. The relative contribution figures can also be found in the fourth column of Table III. An interesting example shows that 'unusable' channels are discarded

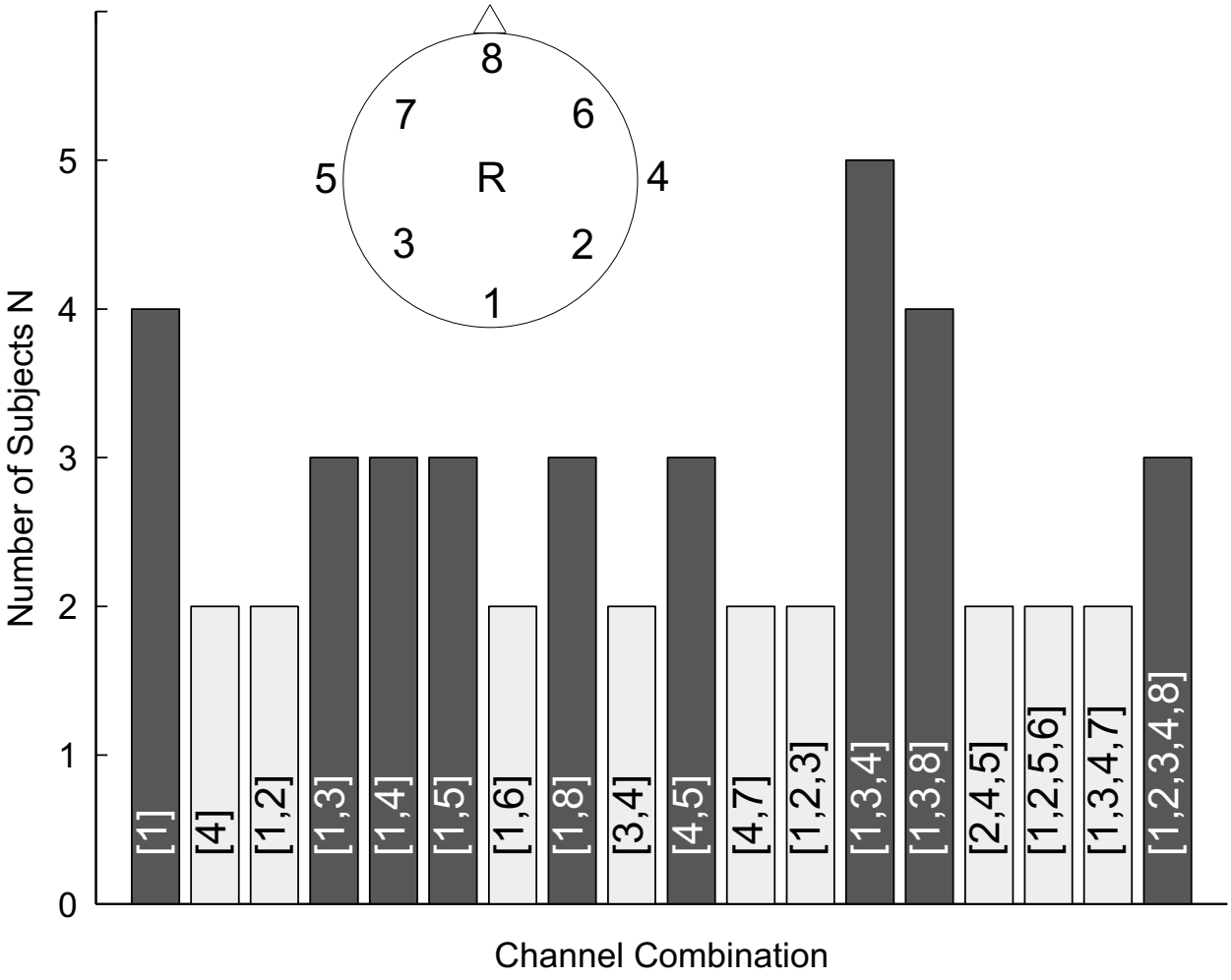

FIG. 2. Channel combinations appearing in the top–ten list of more than two subjects are represented by the dark bars. Channel combinations appearing only twice in the lists are displayed using light bars. 56 combinations appear only once and are not shown here. Channels are combined using (20). Only the combinations with the dark bars are withheld as these exceed the upper level $U = 2$ of the 95 % confidence interval of the 95 percentile of the distribution of appearances in top–ten lists, determined using Monte Carlo simulations. The inset represents a scalp viewed from above showing the electrode positions from Table I.

immediately. During the recording of the data in the first (test) session, channel 4 from both subjects 2 and 4 suffered severely from muscle artifacts at the right mastoid. No contribution is allowed for channel 4 in these subjects.

Based on the total relative contribution over all subjects, a ranking can be produced for

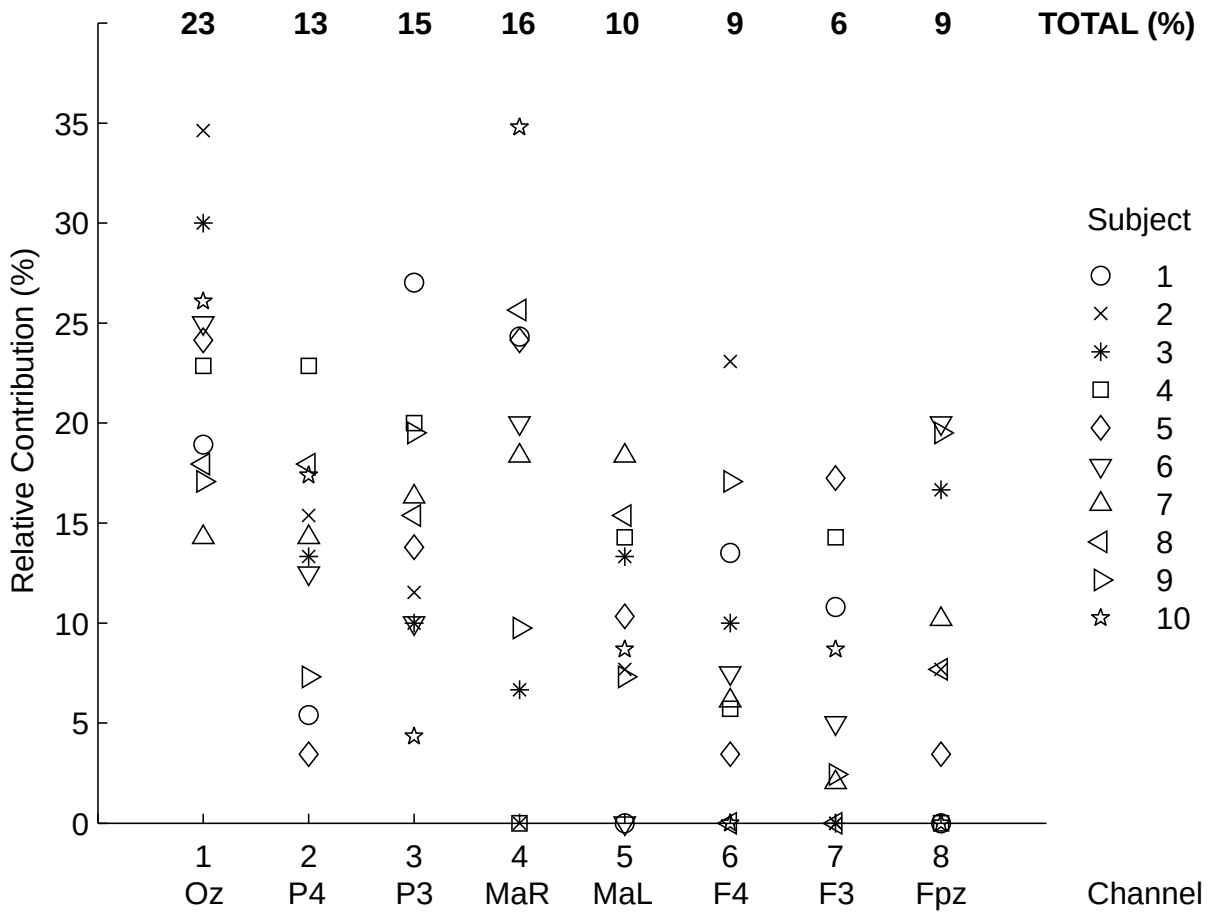

FIG. 3. Relative contribution of each channel to the top–ten list from each subject (and total relative contribution over all subjects). Brainstem responses from both left and right stimulus presentation are used to construct this figure (cf. fourth column of Table III).

the eight channels. For the current derivation the channel ranking is 1 4 3 2 5 6 8 7 (cf. Table III). Guided by this ranking, the minimum number of channels can be determined to cover as many subjects's top–ten lists as possible. The step–by–step construction of this minimum channel set $\mathcal{M}$ is displayed in Table III. The minimum channel set $\mathcal{M}_{80}$ covering at least 80 % of all subjects, is depicted in bold. In the fourth column of Table III, at least one of the seven combinations that can be made from the set $\mathcal{M}_{80} = \{1, 4, 3\}$ will appear in 10 out of 10 (i.e. all) top–ten lists.

When the minimum channel set $\mathcal{M}_{80} = \{1, 4, 3\}$ is determined, the list of withheld combinations ($U > 2$) can be reduced. Channel combinations from this list that can be

formed by $\mathcal{M}_{80}$ are [1] [1,3] [1,4] [1,3,4]. Mean difference scores from these channel combinations range between 18.5 and 19.1 dB (± 1.2 to 1.5 dB). The difference scores of all these combinations are not significantly different and are significantly ($p < 0.05$) pairwise correlated. As a result, any channel selection out of [1] [1,3] [1,4] or [1,3,4] will result statistically in a minimum mean difference score. To be able to select a channel combination that guarantees a difference score that is always in de top–ten of each subject, the three active electrodes should be placed at position 1 (Oz), position 3 (P3), and position 4 (right mastoid), a selection corresponding to minimum set $\mathcal{M}_{80}$. Table IV illustrates this by showing the difference scores of each of these four combinations for each subject, together with their ranking compared with all other combinations within that subject.

c. Splitting up the data in left and right stimulus application

To check whether the asymmetric setup of the previous section is asymmetric for an underlying reason, the available data are split up corresponding to the two sides of stimulation (left or right). In this way, the importance of the side of stimulation for electrode placement is addressed.

Responses originating from stimuli applied to the left ear are considered separately from those resulting from stimuli applied to the right ear. The procedures from Sections IV.A.2.a and IV.A.2.b are repeated identically.

As shown in the second column of Table III, the minimum set $\mathcal{M}_{80}^{L}$ for stimuli applied to the left ear is $\mathcal{M}_{80}^{L} = \{1, 3\}$. This corresponds to active electrodes placed at positions Oz and P3. $\mathcal{M}_{80}^{R} = \{1, 4, 2\}$ is taken as a minimum set $\mathcal{M}_{80}^{R}$ for stimuli applied to the right ear. Active electrodes should be placed at positions Oz, P4, and the right mastoid. In seven of ten subjects, electrodes on the side of stimulation contribute relatively more to the top–ten lists than the contralateral electrodes. In only one subject, this effect is inverted.

The resulting minimum set $\mathcal{M}_{80} = \{1, 4, 3\}$ of the simultaneous stimuli left and right is a combination of the minimum sets $\mathcal{M}_{80}^{L}$ and $\mathcal{M}_{80}^{R}$ of stimuli applied to left and right ear

separately. No apparent reason for the asymmetry in $\mathcal{M}_{80}$ can be found however and can be mainly addressed to the used dataset. When compared with symmetric sets $\{1, 2, 3\}$ and $\{1, 4, 5\}$, the sum of the relative contributions of the single channels from the asymmetric set $\{1, 4, 3\}$ to the top–ten lists is the largest in five of ten subjects. Only in one subject, this sum is the smallest. In the individual subjects, this asymmetry is thus also present.

3. Artifact robustness

Four different processing methods are considered. Two processing methods are single–channel methods. Two methods are multichannel. Channel 1 is taken from Table I as the reference channel for single channel brainstem ASSR measurements with adults (Luts and Wouters, 2005; van der Reijden *et al.*, 2001). Channels 1, 3, and 4 come forward as the minimum set in Section IV.A.2.b and are combined using the multichannel processing scheme from Section II.

The processing schemes are applied on two multichannel EEG datasets obtained at an intensity of 30 dBSPL. Firstly, they are administered on an EEG dataset with few artifacts ('clean EEG') that is identical to the EEG in Section IV.A.1. Secondly, they are applied on an EEG dataset with a considerable number of artifacts ('dirty EEG'), generated as described in Section III.A. To calculate a detection threshold η, each of the four processing methods below are applied on frequencies without a response (e.g. 1 Hz below the modulation frequencies that could contain a response) of the artifact–free multichannel EEG from Section IV.A.1 on all intensities. Then, the 95 percentile of this noise distribution is defined as the detection threshold. In this way four different detection thresholds are obtained for each processing method.

1. *Channel 1, normal averaging.* Channel 1 is divided into 32 sweeps (data blocks of 16.384 seconds) and averaged. Detection is managed using the method described in Section II.D.

2. *Channel 1, noise–weighted averaging.* Each unfiltered epoch (data blocks of 1.024

seconds) is transformed to the frequency domain by using an FFT. The average power P_i between 77 and 115 Hz is computed after removing the power at the 8 frequencies at which responses occurred. The time domain epoch is then weighted with the average power P_i and concatenated with the preceding epochs to form sweeps. Each epoch of the final summed sweep is then divided by the sum of the weights $P = \sum P_i^{-1}$ of the epochs that have been combined to form that particular epoch (adapted from John *et al.* (2001a)). Detection is managed using the method described in Section II.D.

3. Channels 1, 3, and 4 are combined using (20) with $\boldsymbol{K}_{\text{spat}}$ fixed and $\boldsymbol{K}_{\text{temp}} = \sigma I$ fixed. The mean noise power σ^2 is calculated using (23) on the combined channels 1, 3, and 4.

4. Channels 1, 3, and 4 are combined using (22) with $\boldsymbol{K}_{\text{spat}}$ fixed. $\boldsymbol{K}_{\text{temp},i} = P_i P \sigma_n I$ is variable and is recalculated for each block i of 8.192 seconds. This choice of the block size returns the best results. $\boldsymbol{K}_{\text{temp},i}$ is calculated based on the rationale of noise–weighted averaging. P_i is the average power between 77 and 115 Hz of data block i. P is the sum of the reciprocals of P_i, i.e. $P = \sum P_i^{-1}$. The mean noise power σ_n^2 is calculated using (23) on a noise–weighted average of the combined channels 1, 3, and 4.

It is assumed that all responses to the applied stimuli are present in the EEG as the stimulus intensity is 30 dBSPL and hence well above the subject's hearing thresholds. There are thus 16 responses for each of the ten subjects (test and retest) available for detection. The maximum number of detections is 160. Table V shows the number of detections for each approach for EEG with few artifacts ('clean EEG') and EEG with a significant number of artifacts ('dirty EEG'). Test and retest data are not significantly different for both datasets ($p \geq 0.67$).

For EEG with few artifacts, best results are obtained when a noise–weighted averaging approach is used. The improvement relative to normal averaging is not significant however. It does not make a difference if multiple channels are used for processing or just one

(reference) channel.

Response detection in EEG with numerous artifacts is improved significantly when using more than one channel for processing. This improvement can increase significantly when using a noise–weighted averaging based approach.

In Section V, it is discussed whether a symmetric minimum set would give a more logical electrode placement compared with an asymmetric minimum set. Therefore, for illustrative purposes, Table V adds four extra lines showing the multichannel processing results of symmetric minimum sets $\{1, 2, 3\}$ and $\{1, 4, 5\}$.

B. Auditory cortex stimulation

This section will present results from stimulation at only one ear. Six out of ten subjects are stimulated at the right ear. To preserve symmetry, all electrode positions of the other four subjects are mirrored as if stimulation occurred at the right ear. This swapping operation is allowed as no significant difference ($p = 0.904$) in SNR between groups with left ear stimulation and right ear stimulation is found. As a result, Table I refers for this section to the (corrected) side of stimulation as 'ipsilateral' and the opposite side as 'contralateral'.

1. Separate channels

Figure 4 shows the mean SNR (and standard deviation) of the 10 Hz response in all eight channels from Table I for intensities of 50 and 70 dBSPL. Test and retest data are averaged per subject ($p = 0.314$, no interactions). There is no significant difference between both intensities ($p = 0.113$, no interactions). A main effect between channels is present ($p = 0.003$, no interactions). When comparing pairwise (Bonferroni correction) in Figure 4 at 50 dBSPL, the SNRs of channels 4 and 5 are significantly larger than those of channels 6, 7, and 8. Channel 1 is significantly different from channels 6 and 7 and channel 3 only is significantly different from channel 7. At 70 dBSPL, only the SNRs of channel 4 are significantly larger than those of channels 7 and 8. Between subjects an interaction is

present with the EEG channels ($p = 0.044$). This indicates that the EEG channel with the largest SNR for one subject is not necessarily the channel with the largest SNR for another subject. The best EEG channel is subject dependent.

Due to the high variability of the SNRs, it is difficult to identify an optimal electrode placement from Table I in the case of three electrodes available for placement. From the pairwise comparisons above, channels 4 and 5 (both mastoids) appear to be good choices.

2. Combination of channels

Although no significant difference is present between both intensities in the previous subsection, only the results obtained at 50 dBSPL is focused on. The structure of this section is similar to the structure of Section IV.A. Results at 70 dBSPL are similar and will only be described briefly whenever different from those at 50 dBSPL.

In Section IV.A, difference scores between the ASSR threshold and the behavioral threshold were used to quantify performance. As no behavorial data at the stimuli are available, only signal–to–noise ratios are used in the analysis, with a minor modification. A response of e.g. 12 dB resulting from a five–channel combination does not perform as well as a 12 dB response from a three–channel combination. As a result, the concept of corrected SNR appears to be applicable here. The *corrected SNR* is the difference between the response SNR and a threshold SNR. This latter value increases when more channels are added for combination. The *threshold SNR* is determined as the SNR that allows 5 % false detections when observing a frequency bin without any response present (e.g. 1 Hz below the stimulus frequency of 10 Hz). For calculation of the noise estimate, frequency bins with a response are removed.

Again, all 255 combinations of the eight EEG channels in Table I are subject to analysis. Channels are combined using (20) from Section II. No significant difference between the corrected SNRs of test and retest data is found ($p = 0.805$). Therefore, for each subject an average corrected SNR is available for the 10 Hz response and per combination (10×255

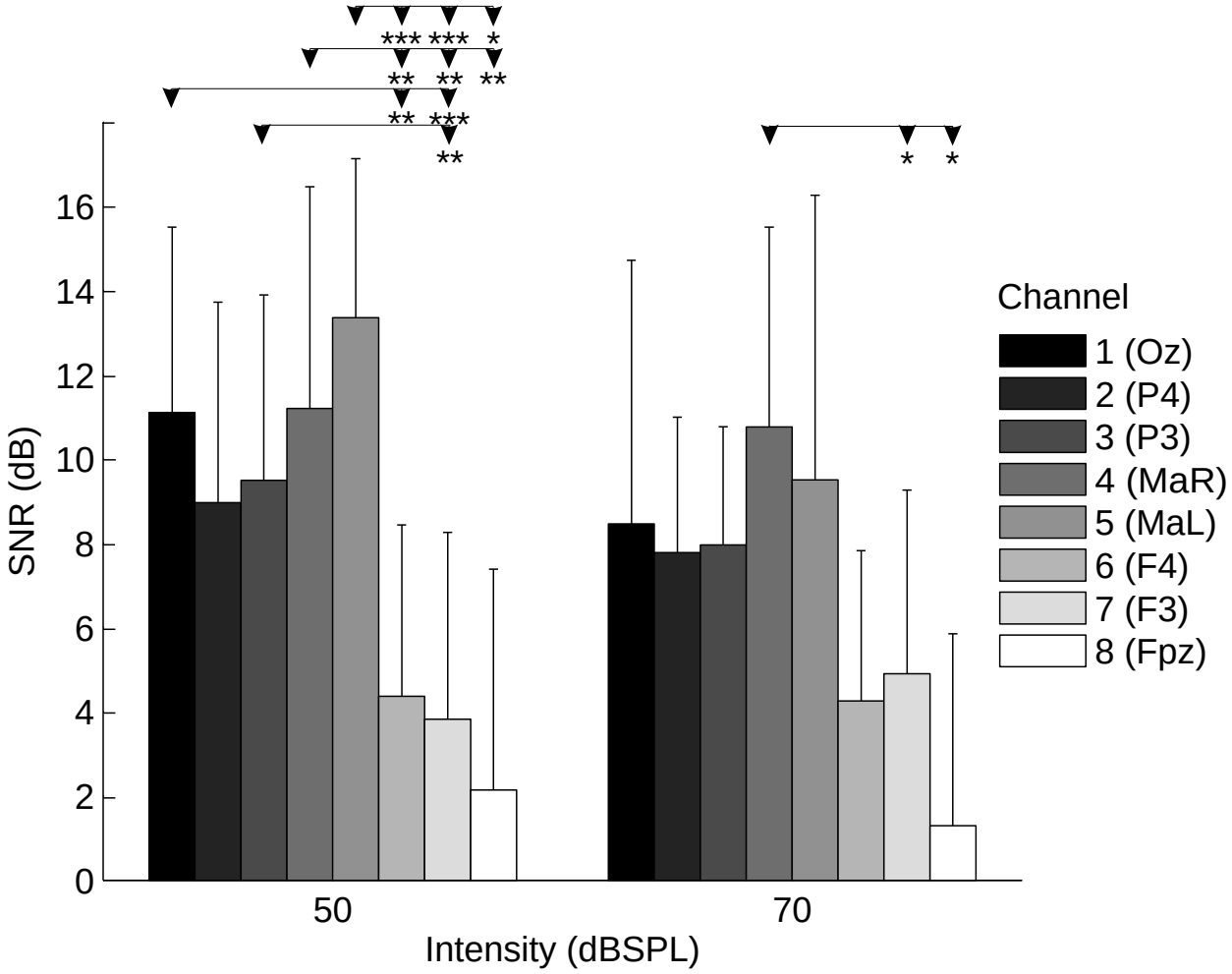

FIG. 4. For stimulus intensities 50 and 70 dBSPL, the mean SNR (and standard deviation) of the 10 Hz response is displayed per channel from Table I. Stimulus application is at the right ear (next to channel 4). Above each intensity, a comparison between channels is displayed. If a statistical difference is present, this is indicated with * ($0.05 > p \geq 0.01$), ** ($0.01 > p \geq 0.001$), and *** ($0.001 > p$).

corrected SNRs in total). The corrected SNRs of most combinations do not have a normal distribution across subjects. Therefore, again a top–ten list is made for each of ten subjects. Zero ties are included. The top–ten list thus contains 100 combinations. The number of times a combination appears in this top–ten list is counted (with a mean chance level of $\bar{d} = \frac{100}{255} = 0.392$). All combinations appearing more than $U = 2$ times in the top–ten list (U as a result of Monte Carlo simulations), are considered not appearing by chance ($p = 0.05$),

with a confidence of 95 %. The withheld combinations for the 10 Hz ASSR are: [5] [1,5] [4,6] [5,7] [2,5,7] [4,5,7] [5,6,7] [5,7,8] [2,5,7,8] [5,6,7,8] [4,5,6,7,8] [2,4,5,6,7,8]. They are also displayed in the fifth column of Table III. Only combinations [5] [5,7] [2,5,7] [5,7,8] can also be found in both test and retest results. To guarantee test–retest reproducibility, the focus is on the individual channels appearing in these combinations instead.

According to the fifth column of Table III, channels 5 and 7 are by far the channels with highest occurence in the subjects's top–ten lists. By adding channels 6 and 8, 90 % of all subjects are covered. The minimum channel set is thus $\mathcal{M}_{80} = \{5, 7, 6, 8\}$. However, when following the channel ranking of Table III exactly, the minimum set $\{5, 7, 6, 4\}$ should be the first choice. This minimum set offers the same amount of coverage as $\{5, 7, 6, 8\}$, but combination [5,7,6,4] does not appear in the list of withheld combinations however, so channel 8 is chosen instead, and consequently for minimum set $\{5, 7, 6, 8\}$.

Based on the minimum channel set $\mathcal{M}_{80}$, only channel combinations [5] [5,7] [5,6,7] [5,7,8] [5,6,7,8] are considered from the list with withheld combinations. Their mean corrected SNRs are between 8.2 and 9.0 dB ($\pm$ 1.1 and 1.2 dB) and not significantly different. They are all significantly pairwise correlated ($p < 0.05$). As a result, any channel selection out of these five combinations will result statistically in a maximum mean corrected SNR. To be able to select a channel combination that guarantees a corrected SNR that is always in de top–ten of each subject, however, the four active electrodes should be placed at position 5 (contralateral mastoid), position 6 (F4), position 7 (F3), and position 8 (forehead). When the data obtained at 70 dBSPL is analyzed, a coverage of 80 % is possible with $\mathcal{M}_{80} = \{5, 7, 6, 4\}$, which is similar to the results at 50 dBSPL.

V. DISCUSSION

All combinations of EEG channels in this paper are processed using a sufficient statistic that theoretically captures best the amount of useful ASSR target signal present in these EEG channels. This sufficient statistic originates from the realm of detection theory (Green

and Swets, 1966). It can be linked with the multichannel Wiener filter (MWF), an optimal filtering technique which computes an optimal (minimum mean square error) estimate of a reference signal (Scharf, 1991). In the case of ASSR detection, this comes down to a maximization of the signal–to–noise ratio of the combined channels (Simmer *et al.*, 2001; Van Dun *et al.*, 2007b). This point of view makes it easier to get an idea of what happens when combining EEG data using (20).

Adding extra data channels will increase the amount of information that is gathered in the same time period. However, to combine these channels, the use of more advanced signal processing is necessary to truly achieve a performance improvement. If multichannel data is combined using e.g. simple time domain averaging over channels, the statistical multiple testing penalty will increase the number of false detections proportionally to the number of extra correct detections. By intelligently combining these channels, this multiple testing problem can partly be avoided.

This section will discuss the results from the previous section for mainly stimulating the brainstem (modulation frequencies between 80 and 110 Hz) and the auditory cortex (10 Hz) respectively.

A. Brainstem stimulation

The transition from the clinical approach of difference scores to the practical quantitative measures of signal–to–noise ratios seems to be allowed due to the high correlations between both measures. It is assumed that results for one measure can be used for the interpretation of the results of the other measure.

When observing the difference scores of reference channel 1 (Cz–Oz), two observations can be made. First, difference scores are slightly elevated compared to other studies. Standard deviations are comparable however (Dimitrijevic *et al.*, 2002; Herdman and Stapells, 2001; Luts and Wouters, 2005; Picton *et al.*, 2003). This difference score gap may be caused by the fact that not as much attention has been directed to the placement of all (i.e. more)

electrodes. The determination method of ASSR hearing thresholds also appears to be rather strict in this study. However, this determination method is kept identical for the whole study and final conclusions should not be influenced. Second, although not significantly different, carrier frequencies of 500 and 4000 Hz show a trend of having larger difference scores than 1 and 2 kHz at these intensities, which is also observed in other studies (Dimitrijevic *et al.*, 2002; Herdman and Stapells, 2001; Luts and Wouters, 2004; Picton *et al.*, 1998). Both observations suggest the data in this study is representative for general brainstem ASSR measurements.

As already indicated in Section III, several studies focus on the sources of the ASSR with frequencies between 80 and 110 Hz, the frequency region of interest for hearing threshold determination. They conclude that for modulation frequencies above about 75 Hz, most of the ASSR is generated in the brainstem. Above 95 Hz, the source lies entirely in the brainstem. These assumptions seem to support the observations made in this paper. With sources mainly in the brainstem the smallest difference scores (and the largest SNRs consequently) are recorded in electrodes close to the brainstem, on the back of the head and the mastoids. The ipsilateral effect of larger SNRs and smaller difference scores (and thus the optimal combination of electrodes) at the side of stimulus application is partly confirmed by Small and Stapells (2008). They indicate that ASSR amplitudes are significantly smaller at the contralateral side. Difference scores with adults do not differ significantly however. For infants, this ipsilateral effect is reported to be strongly present, both for ASSR amplitudes as ASSR thresholds. This asymmetric effect is also confirmed by van der Reijden *et al.* (2005). This could signify that the orientation of the ASSR sources is stimulus side dependent for adults, and especially dependent in the case of infants. The asymmetrical electrode positioning for binaural stimulation can not be confirmed in literature. The authors assume that the results in this paper are merely due to the used dataset and that a symmetrical electrode placement is preferred. According to Table V, a recommended symmetric minimum set could be $\{1, 4, 5\}$, only slightly reducing the number of detections for EEG with few artifacts as well for EEG with many artifacts. To conclude, van der Reijden *et al.* (2004)

report that a small set of three derivations (Cz–inion combined with the right mastoid–Cz and the left mastoid–Cz, which corresponds to the minimum set $\{1, 4, 5\}$) yields the best SNR in a larger number of adults than would be expected if all derivations were equally efficient. This result is very similar to the one obtained in this study.

Multichannel processing does not significantly improve detection performance when it is applied to EEG that does not contain many artifacts. This shows that most single channel studies using a Cz–inion or Cz–neck electrode configuration likely get close to the best obtainable result (for an extensive overview, we refer to Picton *et al.* (2003)). The EEG in these studies is mostly obtained from relaxing adults and sedated children. Studies that specifically incorporate EEG with numerous artifacts are rare however. Unfortunately, these situations reflect the conditions observed mostly in a clinical environment. The proposed technique is significantly more robust against artifacts and may improve measurements in these difficult conditions.

B. Auditory cortex stimulation

As already indicated in Section III, when lowering the modulation frequency of the stimulus, the main source of the ASSR shifts more to the auditory cortex, while still having a source in the brainstem. This may explain the SNRs being largest on the electrodes close to the brainstem (back of the head) and the auditory cortices (both mastoids).

Although no significant differences in SNR are found in Figure 4 between the single electrodes at the ipsilateral and the contralateral mastoid (also reported by Herdman *et al.* (2002)), the dominant channel (contralateral mastoid, channel 5) of the minimum set $\{5, 7, 6, 8\}$ clearly is located at the opposite side of stimulation. This could be explained by the crossing of the auditory paths beyond the brainstem (Hall, 1992). The extra channels 6, 7, and 8 of the minimum set $\{5, 7, 6, 8\}$ lie at the front of the head, in contrast with the channels with the largest SNRs lying at the back of the head as shown in Figure 4. This can be explained by the underlying mechanism of the multichannel processing technique from

Section II. The result of the weighted channels has theoretically the largest possible SNR (Van Dun *et al.*, 2007b, 2008a). For responses originating mainly from the auditory cortex, this result is likely obtained by taking the channel with the largest response (channel 5), and by adding channels that have a small response (channels 6, 7, and 8) and that have a high noise correlation with the noise in the channel with the largest response. This observation is in contrast with the conclusions in Section V.A, that locates the minimum set $\{1, 4, 2\}$ in the back of the head for responses originating mainly from the brainstem. The dominant channel for this minimum set is the inion (channel 1). Any additional channels with small responses (channels 6, 7, and 8 in front of the head according to Figure 1) appear to be too remote as noise correlation with these remote channels is presumably too low in the frequency region of interest (80 – 110 Hz).

The trend in observing smaller SNRs for higher intensities of stimulation is in agreement with Hall (1992) where it is stated that 'maximum response typically is obtained for moderate (50–60 dB) versus high–intensity stimuli'.

VI. CONCLUSION

In this paper, the practical performance of a multichannel EEG processing strategy for ASSR detection based on a detection theory approach is evaluated. Eight–channel measurements of ten normal–hearing adults have been used. First, ASSRs with modulation frequencies between 80 and 110 Hz and mainly originating from the brainstem are considered. It is shown that electrodes should be placed at the back of the head and at the mastoids to obtain the largest mean SNRs and the smallest mean difference scores for individual electrodes. When applying the multichannel processing strategy, the smallest difference scores are found with all subjects when electrodes are placed at five positions: Oz, P3, and right mastoid with Cz as a reference electrode and a ground electrode at e.g. the right clavicle. This combination is significantly more robust against artifacts when compared with a single channel, three electrode, setup. The number of ASSR detections is more than doubled when

EEG with artifacts is considered. Second, ASSRs with a modulation frequency of 10 Hz and mainly originating from the auditory cortex are studied. Again, the largest mean SNRs are obtained at single electrodes located at the back of the head and at both mastoids. When applying multichannel processing, the largest mean SNRs for minimum 80% of the subjects are obtained when placing electrodes at the contralateral mastoid, F4, F3, and the forehead with Cz as a reference electrode and a ground electrode at e.g. the right clavicle.

Acknowledgments

This work was supported in part by the Institute for the Promotion of Innovation through Science and Technology in Flanders (IWT–Vlaanderen); in part by FWO project G.0504.04 ("Design and analysis of signal processing procedures for objective audiometry in newborns"); and in part by the Concerted Research Action GOA–AMBioRICS.

References

Armstrong, M. and Stapells, D. R. (**2007**). "Multiple–stimulus interactions in the brainstem (80 Hz) and cortical (14 & 40 Hz) auditory steady–state responses", in *Proc. of the 20th International Evoked Response Audiometry Study Group (IERASG)*, 148 (Bled, Slovenia).

Cebulla, M., Stürzebecher, E., and Elbering, E. (**2006**). "Objective detection of auditory steady–state responses: comparison of one–sample and q–sample tests", J. Am. Ac. Audiol. **17**, 93–103.

Cebulla, M., Stürzebecher, E., and Wernecke, K. D. (**2001**). "Objective detection of the amplitude modulation following response (AMFR)", Audiology **40**, 245–252.

Dimitrijevic, A., John, M. S., Van Roon, P., Purcell, D. W., Adamonis, J., Ostroff, J., Nedzelski, J. M., and Picton, T. W. (**2002**). "Estimating the audiogram using auditory steady–state responses", J. Am. Ac. Audiol. **13**, 205–224.

Dobie, R. A. and Wilson, M. J. (**1996**). "A comparison of t test, f test, and coherence methods of detecting steady–state auditory–evoked potentials, distortion–product otoacoustic

emissions, or other sinusoids", J. Acoust. Soc. Am. **100**, 2236–2246.

Galambos, R., Makeig, S., and Talmachoff, P. J. (**1981**). "A 40–Hz auditory potential recorded from the human scalp", Proc. Natl. Acad. Sci. USA **78**, 2643–2647.

Green, D. and Swets, J. A. (**1966**). *Signal detection theory and psychophysics* (New York: John Wiley & Sons Inc).

Hall, J. W. (**1992**). *Handbook of auditory evoked responses* (Boston: Allyn and Bacon).

Herdman, A. T., Lins, O., Van Roon, P., Stapells, D. R., Scherg, M., and Picton, T. W. (**2002**). "Intracerebral sources of human auditory steady–state responses", Brain Topogr. **15**, 69–86.

Herdman, A. T. and Stapells, D. R. (**2001**). "Thresholds determined using the monotic and dichotic multiple auditory steady–state response technique in normal–hearing subjects", Scand. Audiol. **30**, 41–49.

Hyvärinen, A., Karhunen, J., and Oja, E. (**2001**). *Independent component analysis* (New York: John Wiley & Sons Inc).

John, M. S., Dimitrijevic, A., and Picton, T. W. (**2001a**). "Weighted averaging of steady state responses", Clin. Neurophysiol. **122**, 555–562.

John, M. S., Dimitrijevic, A., and Picton, T. W. (**2002**). "Auditory steady–state responses to exponential modulation envelopes", Ear Hear. **23**, 106–117.

John, M. S., Dimitrijevic, A., and Picton, T. W. (**2003**). "Efficient stimuli for evoking auditory steady–state responses", Ear Hear. **24**, 406–423.

John, M. S., Dimitrijevic, A., Van Roon, P., and Picton, T. W. (**2001b**). "Multiple auditory steady–state responses to AM and FM stimuli", Audiol. Neuro-Otol. **6**, 12–27.

John, M. S. and Picton, T. W. (**2000**). "MASTER: a Windows program for recording multiple auditory steady–state responses", Comput. Methods Programs Biomed. **61**, 125–150.

Johnson, D. H. and Dudgeon, D. E. (**1993**). *Array Signal Processing: Concepts and Techniques* (London: Prentice–Hall).

Joint Committee on Infant Hearing (**1995**). "Joint committee on infant hearing 1994 position

statement. American academy of pediatrics joint committee on infant hearing", Pediatrics **95**, 152–156.

Kuwada, S., Anderson, J. S., Batra, R., Fitzpatrick, D. C., Teissier, N., and D'Angelo, W. R. (**2002**). "Sources of the scalp recorded amplitude–modulation following response", J. Am. Ac. Audiol. **13**, 188–204.

Lins, O. G. and Picton, T. W. (**1995**). "Auditory steady–state responses to multiple simultaneous stimuli", Electroencephalogr. Clin. Neurophysiol. **96**, 420–432.

Luts, H., Desloovere, C., and Wouters, J. (**2006**). "Clinical application of dichotic multiple–stimulus auditory steady–state responses in high–risk newborns and young children", Audiol. Neuro-Otol. **11**, 24–37.

Luts, H. and Wouters, J. (**2004**). "Hearing assessment by recording multiple auditory steady–state responses: the influence of test duration", Int. J. Audiol. **43**, 471–478.

Luts, H. and Wouters, J. (**2005**). "Comparison of MASTER and AUDERA for measurement of auditory steady–state responses", Int. J. Audiol. **44**, 244–253.

Malmivuo, J. and Plonsey, R. (**1995**). *Bioelectromagnetism: principles and applications of bioelectric and biomagnetic fields* (New York: Oxford University Press).

Picton, T. W., Durieux-Smith, A., Champagne, S. C., Whittingham, J., Moran, L. M., Giguere, C., and Beauregard, Y. (**1998**). "Objective evaluation of aided thresholds using auditory steady–state responses", J. Am. Ac. Audiol. **9**, 315–331.

Picton, T. W., John, M. S., Dimitrijevic, A., and Purcell, D. (**2003**). "Human auditory steady–state responses", Int. J. Audiol. **42**, 177–219.

Press, W. H., Flannery, B. P., Teukolsky, S. A., and Vetterling, W. T. (**1992**). *Confidence Limits on Estimated Model Parameters in* Numerical Recipes in C, chapter 15.6, 689–698 (Cambridge: Cambridge University Press).

Purcell, D. W., John, M. S., Schneider, B. A., and Picton, T. W. (**2004**). "Human temporal auditory acuity as assessed by envelope following responses", J. Acoust. Soc. Am. **116**, 3581–3593.

Riquelme, R., Kuwada, S., Filipovic, B., Hartung, K., and Leonard, G. (**2006**). "Optimizing

the stimuli to evoke the amplitude modulation following response (AMFR) in neonates", Ear Hear. **27**, 104–119.

Scharf, L. L. (**1991**). *Statistical signal processing : Detection, estimation and time series analysis*, 1st edition (New York: Addison Wesley).

Shannon, R. V., Zeng, F. G., Kamath, V., Wygonski, J., and Ekelid, M. (**1995**). "Speech recognition with primarily temporal cues", Science **270**, 303–304.

Simmer, K. U., Bitzer, J., and Marro, C. (**2001**). *Post–filtering techniques in* Microphone Arrays: Signal Processing Techniques and Applications, chapter 3, 39–60 (M. Brandstein, D. Ward (eds.), Berlin: Springer–Verlag).

Small, S. A. and Stapells, D. R. (**2008**). "Normal ipsilateral/contralateral asymmetries in infant multiple auditory steady–state responses to air– and bone–conduction stimuli", Ear Hear. **29**, 185–198.

Stürzebecher, E., Cebulla, M., Elberling, C., and Berger, T. (**2006**). "New efficient stimuli for evoking frequency–specific auditory steady–state responses", J. Am. Ac. Audiol. **17**, 448–461.

Stürzebecher, E., Cebulla, M., and Pschirrer, U. (**2001**). "Efficient stimuli for recording of the amplitude modulation following response", Audiology **40**, 63–68.

Valdes, J. L., Perez-Abalo, M. C., Martin, V., Savio, G., Sierra, C., Rodriguez, E., and Lins, O. (**1997**). "Comparison of statistical indicators for the automatic detection of 80 Hz auditory steady state responses", Ear Hear. **18**, 420–429.

van der Reijden, C. S., Mens, L. H. M., and Snik, A. F. M. (**2001**). "Comparing signal–to–noise ratios of amplitude modulation following responses from four EEG derivations in awake normally hearing adults", Audiology **40**, 202–207.

van der Reijden, C. S., Mens, L. H. M., and Snik, A. F. M. (**2004**). "Signal–to–noise ratios of the auditory steady–state response from fifty–five EEG derivations in adults", J. Am. Ac. Audiol. **15**, 692–701.

van der Reijden, C. S., Mens, L. H. M., and Snik, A. F. M. (**2005**). "EEG derivations providing auditory steady–state responses with high signal–to–noise ratios in infants", Ear

Hear. **26**, 299–309.

Van Dun, B., Rombouts, G., Wouters, J., and Moonen, M. (**2008**a). "A procedural framework for auditory steady–state response detection", in *Technical Report 08–99, ESAT–SISTA, Katholieke Universiteit Leuven, Belgium* (Submitted for publication).

Van Dun, B., Verstraeten, S., Alaerts, J., Luts, H., Moonen, M., and Wouters, J. (**2008**b). "A flexible research platform for multi–channel auditory steady–state response measurements", J. Neurosci. Meth. **169**, 239–248.

Van Dun, B., Wouters, J., and Moonen, M. (**2007**a). "Improving auditory steady–state response detection using independent component analysis on multi–channel EEG data", IEEE Trans. Biomed. Eng. **54**, 1220–1230.

Van Dun, B., Wouters, J., and Moonen, M. (**2007**b). "Multi–channel Wiener filtering based auditory steady–state response detection", in *Proc. of the International Conference on Acoustics, Speech and Signal Processing (ICASSP)*, volume II, 929–932 (Honolulu, HI, USA).

Van Wieringen, A. and Wouters, J. (**2008**). "LIST and LINT: Sentences and numbers for quantifying speech understanding in severly impaired listeners for Flanders and the Netherlands", Int. J. Audiol. **47**, 348–355.

TABLE I. Recording electrode positions for an eight–channel setup according to the international 10–20 system (Malmivuo and Plonsey, 1995). All channels are referenced to the reference electrode on top of the head (Cz). A graphical representation is shown in Figure 2. The term 'Side' indicates on which hemisphere of the head the electrode is placed in the case it is not positioned on the middle line from front to back. In general, the sides can be 'Left' or 'Right'. However, for ASSRs from the auditory cortex, being described in Section IV.B (with stimuli referenced to the right ear), one refers to the sides as 'Ipsilateral' and 'Contralateral'. The ipsilateral side is the side of stimulation.

Channel	Position	Side
1	inion (Oz)	
2	P4	R / I
3	P3	L / C
4	right mastoid (MaR)	R / I
5	left mastoid (MaL)	L / C
6	F4	R / I
7	F3	L / C
8	forehead (Fpz)	
reference	vertex (Cz)	
ground	right clavicle	

TABLE II. For each channel from Table I, the mean SNRs (and standard deviations between brackets) of the modulation frequencies modulating the corresponding carrier frequency (500, 1000, 2000, and 4000 Hz, left and right) at a stimulus level of 30 dBSPL are displayed. The mean RMS values (and standard deviations) of the noise of each channel are depicted on the right of the table.

Channel	Left (dB SNR)				Right (dB SNR)				RMS (nV)
number	500 Hz	1000 Hz	2000 Hz	4000 Hz	500 Hz	1000 Hz	2000 Hz	4000 Hz	
1 (Oz)	5.1 (6.5)	9.3 (2.8)	8.3 (4.0)	5.9 (6.3)	7.1 (5.2)	9.5 (7.0)	10.2 (3.9)	6.8 (5.6)	4.0 (1.3)
2 (P4)	4.2 (5.9)	5.8 (5.4)	4.9 (4.6)	3.1 (5.6)	5.9 (6.7)	9.7 (7.1)	10.1 (3.1)	6.0 (5.1)	2.5 (0.6)
3 (P3)	5.5 (4.7)	8.5 (4.6)	7.9 (4.1)	4.7 (4.9)	4.1 (5.3)	5.6 (6.3)	2.1 (5.4)	-0.4 (4.5)	2.7 (0.6)
4 (MaR)	3.8 (7.6)	7.7 (5.0)	4.6 (6.6)	3.6 (7.0)	7.4 (7.7)	12.0 (5.5)	9.9 (2.5)	6.8 (4.7)	7.1 (3.1)
5 (MaL)	4.5 (7.6)	10.2 (4.8)	8.1 (6.8)	5.1 (5.7)	4.5 (6.1)	7.2 (6.5)	8.7 (4.4)	3.4 (5.1)	6.1 (1.9)
6 (F4)	0.9 (2.2)	1.8 (5.0)	-0.5 (2.5)	-0.3 (4.7)	2.5 (3.1)	4.6 (4.5)	5.4 (3.0)	0.7 (3.2)	4.9 (3.0)
7 (F3)	2.5 (3.0)	5.0 (5.7)	1.9 (8.6)	0.5 (6.4)	3.0 (4.6)	3.9 (5.5)	2.9 (6.8)	0.6 (5.5)	3.7 (1.8)
8 (Fpz)	0.1 (4.8)	2.7 (5.1)	0.9 (5.1)	-1.3 (5.0)	1.8 (6.9)	3.5 (4.2)	3.3 (4.8)	0.7 (3.0)	4.9 (2.6)

TABLE III. Step–by–step derivation of most optimal electrode combination for responses originating mainly from the brainstem and mainly from the auditory cortex.

	BRAINSTEM (80 – 110 Hz)			CORTEX (10 Hz)
	Left	Right	Combined	
Selected combinations ($U > 2$)	**[1][1,3]**[1,4] [1,5][1,8][4,5] [1,3,4][1,3,8]	**[1][2][4]** **[1,2][2,4]**[3,4] [4,7]**[1,2,4]**	**[1][1,3][1,4]**[1,5] [1,8][4,5]**[1,3,4]** [1,3,8][1,2,3,4,8]	**[5]**[1,5][4,6]**[5,7]** [2,5,7][4,5,7]**[5,6,7]** **[5,7,8]**[2,5,7,8]**[5,6,7,8]** [4,5,6,7,8][2,4,5,6,7,8]
Relative contribution (%)	22 11 17 16 13 6 7 8	19 16 12 18 9 11 7 8	23 13 15 16 10 9 6 9	6 10 6 12 25 12 18 11
Channel ranking	1 3 4 5 2 8 7 6	1 4 2 3 6 5 8 7	1 4 3 2 5 6 8 7	5 7 6 4 8 2 3 1
Minimum sets $\mathcal{M}$	$\{1\}$ – 5 **$\{1,3\}$ – 9** $\{1,3,8\}$ – 10	$\{1\}$ – 3 $\{1,4\}$ – 7 **$\{1,4,2\}$ – 8** $\{1,4,2,3\}$ – 9 $\{1,4,2,3,6\}$ – 10	$\{1\}$ – 4 $\{1,4\}$ – 7 **$\{1,4,3\}$ – 10**	$\{5\}$ – 5 $\{5,7\}$ – 6 $\{5,7,6\}$ – 7 **$\{5,7,6,8\}$ – 9** $\{5,7,6,8,2\}$ – 10
Recommended electrodes based on this dataset	{1,3}	{1,4,2}	{1,4,3}	{5,7,6,8}

TABLE IV. Difference scores (dB) averaged over all eight frequencies for six relevant combinations, with their ranking (between brackets) compared with all other combinations within the same subject. The six combinations displayed are the best (smallest difference score) and the worst combination, and the four combinations selected in Section IV.A.2.b. Combinations that were in a subject's top–ten, are highlighted in bold.

Subject	1	2	3	4	5	6	7	8	9	10
Best	14.4 (1)	20.9 (1)	18.1 (1)	13.1 (1)	13.1 (1)	12.5 (1)	16.9 (1)	20.3 (1)	18.4 (1)	10.0 (1)
[1]	21.9 (154)	**22.8 (9)**	**18.1 (1)**	17.5 (58)	14.4 (11)	17.5 (44)	19.3 (83)	25.3 (194)	**20.9 (10)**	**10.0 (1)**
[1, 3]	**14.4 (1)**	23.4 (15)	**19.4 (3)**	**13.8 (3)**	15.6 (52)	19.4 (114)	20.0 (134)	23.4 (91)	22.2 (35)	13.8 (23)
[1, 4]	20.0 (83)	22.8 (12)	20.6 (13)	20.0 (145)	14.4 (12)	**15.0 (6)**	**18.1 (9)**	22.2 (27)	24.1 (108)	**11.3 (4)**
[1, 3, 4]	**16.3 (6)**	25.9 (90)	**20.0 (6)**	18.8 (103)	**13.8 (6)**	17.5 (47)	18.1 (15)	**20.9 (3)**	27.2 (188)	**12.5 (10)**
Worst	41.3 (255)	37.2 (255)	53.8 (255)	30.0 (255)	29.4 (255)	33.8 (255)	41.9 (255)	45.9 (255)	52.2 (255)	42.5 (255)

TABLE V. Number of detections (with a maximum of 160) for each processing method when applied to EEG with few artifacts ('clean EEG') and EEG with a significant number of artifacts ('dirty EEG'). For methods 1, 2, 3, and 4, comparisons have been conducted pairwise with Bonferroni correction. Methods 3', 3", 4', and 4" process two symmetric channel sets, but are not used for the pairwise comparisons. They are only placed in this table for illustrative purposes.

Method	Description	Clean EEG	Dirty EEG
1	Normal averaging channel 1	117	17
2	Weighted averaging channel 1	122	35
3	$\boldsymbol{K}_{\text{temp}} = \sigma I$ fixed; [1,3,4]	117	57[a]
4	$\boldsymbol{K}_{\text{temp},i} = P_i P \sigma_n I$ var; [1,3,4]	**122**	**72**[b]
3'	$\boldsymbol{K}_{\text{temp}} = \sigma I$ fixed; [1,2,3]	113	31
4'	$\boldsymbol{K}_{\text{temp},i} = P_i P \sigma_n I$ var; [1,2,3]	122	50
3"	$\boldsymbol{K}_{\text{temp}} = \sigma I$ fixed; [1,4,5]	108	44
4"	$\boldsymbol{K}_{\text{temp},i} = P_i P \sigma_n I$ var; [1,4,5]	112	66

[a]Significantly better than approach 1 ($p < 0.01$).

[b]Significantly better than approach 1 ($p < 0.001$), approach 2 ($p < 0.01$), and approach 3 ($p < 0.05$).

List of Figures

FIG. 1 For each channel from Table I, the mean difference scores (and standard deviations) are displayed for all modulated carriers (500, 1000, 2000, and 4000 Hz, left and right). Above each cluster of bars, the relation between carriers applied to the left ear (L) and the right ear (R) is shown. Under each cluster of bars, a comparison between channels is displayed. If a statistical difference is present, this is indicated with * ($0.05 > p \geq 0.01$) and ** ($0.01 > p \geq 0.001$). A trend is considered present if $0.1 > p \geq 0.05$. 17

FIG. 2 Channel combinations appearing in the top–ten list of more than two subjects are represented by the dark bars. Channel combinations appearing only twice in the lists are displayed using light bars. 56 combinations appear only once and are not shown here. Channels are combined using (20). Only the combinations with the dark bars are withheld as these exceed the upper level $U = 2$ of the 95 % confidence interval of the 95 percentile of the distribution of appearances in top–ten lists, determined using Monte Carlo simulations. The inset represents a scalp viewed from above showing the electrode positions from Table I. 21

FIG. 3 Relative contribution of each channel to the top–ten list from each subject (and total relative contribution over all subjects). Brainstem responses from both left and right stimulus presentation are used to construct this figure (cf. fourth column of Table III). 22

FIG. 4 For stimulus intensities 50 and 70 dBSPL, the mean SNR (and standard deviation) of the 10 Hz response is displayed per channel from Table I. Stimulus application is at the right ear (next to channel 4). Above each intensity, a comparison between channels is displayed. If a statistical difference is present, this is indicated with * ($0.05 > p \geq 0.01$), ** ($0.01 > p \geq 0.001$), and *** ($0.001 > p$). 28